JOURNAL OF MATERIALS SCIENCE **38** (2003) 4325–4332

The influence of precursor powders and processing parameters on the properties of SnO_2-based gas sensors

A. AHMAD*, J. WALSH
Materials Technology Laboratory CANMET/NRCan, 405 Rochester Street, Ottawa, Ontario, Canada, K1A 0G1
E-mail: aahmad@nrcan.gc.ca

Semiconducting tin oxide precursor powders were synthesized via three different chemical processing routes. The influence of powder processing conditions on the physical properties, e.g., particle size, surface area and phase composition of both uncalcined and calcined materials, was investigated. These powders were used to fabricate gas sensors using thick-film screen-printing technology. The effect of precursor powders, sintering conditions, sensor temperature and Pd catalyst on the carbon monoxide, methane, propane and ethanol gas sensing characteristics of the sensors were investigated. Sensors were also fabricated using tin oxide powders obtained from a commercial source and their gas sensing properties were also investigated. The data indicates that the powder processing methodology, sensor fabrication conditions and Pd catalyst can profoundly influence the physical characteristics as well as the gas sensing properties of the sensors.

1. Introduction

With increasing world population and industrialization, air pollution from transportation, industrial, and residential sources is continually on the rise. The air pollution/greenhouse gas emissions from the above sources is known to cause global warming, acid rain and photochemical smog with resulting damage to the environment and living beings. Intelligent systems based on sensors and controls offer an opportunity to increase the efficiency of energy usage in various combustion systems and reduce the emission of greenhouse gases (GHG) that cause global warming, smog and acid rain. In addition, sensors and controls (S&C's) can be used for process control to improve productivity and product quality in various industrial sectors. Applications exist in air quality monitoring and control, energy efficiency, industrial process control, transportation, health & safety (e.g., to detect toxic, flammable and explosive gases in mines and industrial/residential environments), medical diagnostics, material recycling, etc. There is an ongoing need for the development of fast, sensitive, rugged, reliable and low-cost sensors for applications in harsh environments found in automotive, metallurgical processing, aerospace, glass, ceramics, pulp and paper, energy production/generation, etc. industries. The automotive industry is an excellent example, wherein online oxygen sensors and a three-way catalyst, in conjunction with a microprocessor-based control circuit, provide >10% increase in fuel efficiency and commensurate reduction in GHG's.

Current sensing technologies based on electrochemistry, calorimetry, chromatography and spectroscopic techniques are either too expensive or cumbersome to use. Solid-state gas sensors based on semiconducting materials are attractive because of their low cost, small size, ease of fabrication and compatibility with electronic systems. The electrical properties of most of the semiconducting materials are known to be influenced by the adsorption and/or reaction of various gases in the environment. This property of semiconducting materials is typically exploited in gas sensing measurements. Semiconducting oxide materials such as ZnO, TiO_2, Fe_2O_3, WO_3, and SnO_2 are commonly investigated materials for gas sensing applications. Among these, tin oxide (SnO_2) is perhaps the most widely investigated. It generally behaves as an *n*-type semiconductor (i.e., electrons are majority charge carriers) with a wide band-gap, $\Delta E = 3.6$ eV, due to slight non-stoichiometry which arises from the variable oxidation states of tin [1]. The major drawback with tin dioxide-based semiconducting gas sensors is their non-selectivity, i.e., the inability to provide clearly distinguishable response signals when exposed to a mixture of reducing gases, e.g., CO, CH_4, C_3H_8, H_2, etc. Also, environmental factors such as variations in temperature and humidity can often adversely influence the sensor response [2–6]. These problems can often be resolved by using higher operating temperatures, by adding dopants or other metal oxides to the tin oxide, or by changing the base semiconducting oxide [7–13].

*Author to whom all correspondence should be addressed.

The gas sensing properties of these materials are known to be influenced by the material formulation, precursor raw materials, as well as various fabrication and processing conditions that affect the microstructure of the precursor powders and the gas sensing elements. This report provides data on the tin oxide-based gas sensors prepared from precursor powders synthesized via three different precipitation routes and also those fabricated using commercial tin oxide powders. Precursor powders have been synthesized using both high- and low-concentration solutions of chemical reagents (i.e., $SnCl_4 \cdot 5H_2O$ and NH_4OH) for precipitation reactions. In addition, a homogeneous precipitation method that involves precipitation of $SnCl_4 \cdot 5H_2O$ using a urea solution has also been used for the synthesis of SnO_2 precursor powders. The effect of reagent/solution concentration on the physical properties of precipitated and as-calcined powders, and on the sintered thick-film sensor elements produced from these powders, has been investigated. To our knowledge, no systematic study of the influence of chemical reagents/solution concentrations on the properties of tin oxide precursor powders and sintered sensor elements has been previously reported. Also, even though several semiconducting materials (including SnO_2) have been synthesized via the homogeneous precipitation method to provide high surface area precursor powders, reports on their utilization for gas sensor applications, appear to be absent. The paper also gives detailed information on the synthesis and processing of tin oxide powders via three different chemical processing methods to produce high surface area tin oxide precursor powders. Such details are often missing in the literature. Here, data is provided about the influence of various powder synthesis and processing conditions on the surface area/particle size, phase composition and crystal size (as determined by X-ray diffraction technique) of both uncalcined and calcined materials. The influence of precursor powders, sintering temperature, sintering time, Pd-catalyst, and gas concentration, on the electrical conductance, sensitivity and response/recovery times of the thick-film gas sensors produced from these powders is also discussed.

2. Experimental

2.1. Preparation of precursor powder

Fig. 1 illustrates the preparation of SnO_2 precursor powders synthesized via three different precipitation routes. SnO_2 precursor powders were also obtained from a commercial supplier (Strem Chemicals, USA). The first precipitation method designated here as Sn-HC, used relatively higher concentrations of chemical reagents. For this purpose, 0.52 M aqueous solution of $SnCl_4 \cdot 5H_2O$ was slowly added to 5.85 M NH_4OH solution with constant stirring. The second precipitation process (Sn-LC) involved the use of dilute NH_4OH ($\sim$0.4 M) and $SnCl_4 \cdot 5H_2O$ (0.1 M) solutions. For this purpose, 0.1 M aqueous solution of $SnCl_4 \cdot 5H_2O$ was added dropwise into 1 L of ammonia solution over a period of 1.5 h with constant stirring. The third precipitation process (Sn-HM) is also known as the homogeneous precipitation method [14]. In this process, the precipitation occurs via a highly uniform increase in the pH of the solution and this uniformity is achieved by thermal decomposition of urea according to the following reaction:

$$(NH_2)_2CO + 3H_2O \rightarrow CO_2 + 2NH_4^+ + 2OH^- \quad (1)$$

For the homogeneous precipitation process, 0.5 M urea solution was added dropwise to 0.025 M $SnCl_4 \cdot 5H_2O$ solution with stirring over a 10-min period. The mixture was then heated slowly to 80°C and allowed to react for 4 h. The urea decomposes slowly releasing ammonia and carbonate ions into the solution. The gradual and uniform rise in pH results in nucleation and growth of uniformly-sized and shaped particles of

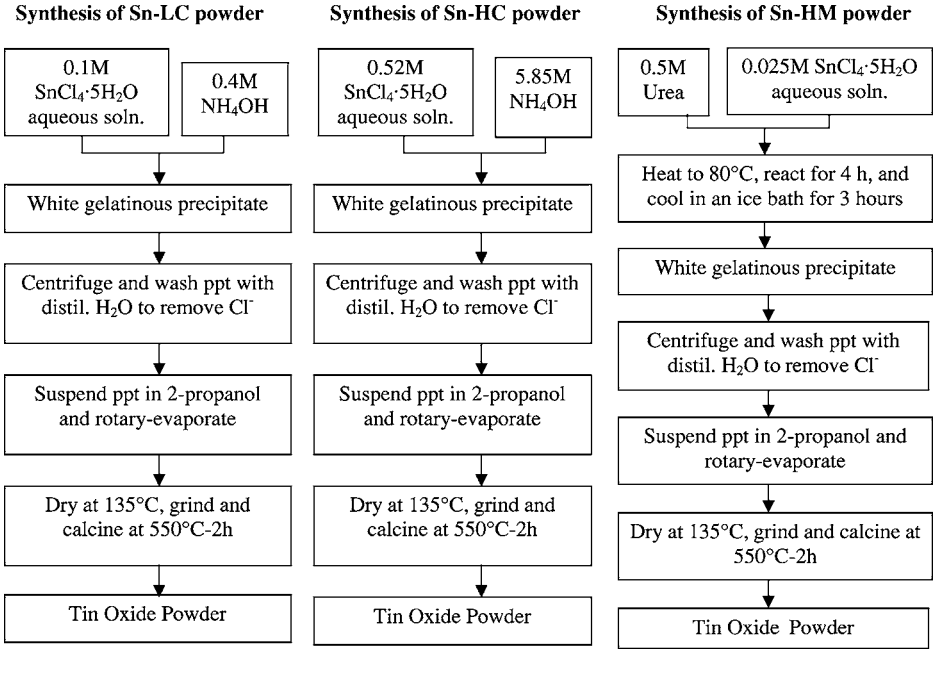

Figure 1 Flow charts for the synthesis and processing of tin oxide powders.

the metal oxy-basic carbonate. The remaining processing steps used to obtain tin oxide precursor powders via the above three processing methods are shown in Fig. 1. The as-calcined powders Sn-LC and also those obtained from a commercial source (Sn-CM) were also impregnated with (0.5–1) mol% Pd-catalyst by attrition-milling the calcined powders for two hours in acetone/isopropanol solution containing the required amount of Pd-acetate dopant. The powders were then rotary-evaporated to remove the solvent and heat-treated in a furnace at 400°C for two hours to decompose the organics.

2.2. Fabrication of sensor elements

The calcined powders obtained by the above three methods as well as those from the commercial supplier were first ground using a mortar and pestle to achieve consistent and fine particles. The sensor fabrication procedure included the sequential screen-printing of inter-digital gold electrodes onto an alumina substrate (25 mm × 25 mm dimension, laser-scribed into 9 equal squares) followed by the superposition of a gas-sensitive layer using an Aremco Accu-Coat 3200 screen printer. The gold inter-digital electrodes (having comb-type structure) were printed on an alumina substrate using gold paste, 3066 Au, obtained from Ferro Inc. These electrodes were fired at 850°C for 10 min using heating and cooling rates of 25°C/min. Electrical contacts to the electrodes were made using platinum wires. The pastes used for the screen-printing of a gas-sensitive layer consisted of the calcined powders produced by the above four methods. These powders were mixed with an organic vehicle (produced in-house by mixing binder, plasticizer, solvent, etc.) in the ratio of 65 wt% powder to 35 wt% organic vehicle. The paste was made using a three-roller mill from Charles Ross & Sons Company. A schematic of the sensor design and the details of the measurement set-up are given elsewhere [15, 16]. The sensing elements produced from each of the four precursor powders were sintered at 725, 775 or 850°C, for a periods of 10, 20 or 30 min using heating and cooling rates of 25°C.

2.3. Materials/sensors characterization

X-ray diffraction (XRD) measurements were carried out to determine the crystal structure or phase composition of the materials. The crystallite sizes (R_x) of the calcined and sintered materials were calculated from the XRD peak broadening of the [110] peak at a diffraction angle of ∼26.55 degrees 2θ using Scherrer's equation [17]:

$$R_x = 0.9\lambda/(\beta \cos\theta) \tag{2}$$

where λ is the wavelength (1.5406 Å for Cu K_α radiation), β is the full-width-half-maximum (FWHM) of a peak in radians and θ is the diffraction angle. The specific surface area of powders was measured by the BET method of nitrogen adsorption using a Quantasorb instrument from Quantachrome Corp. The mean particle size R_m in nanometers (nm) was calculated from surface area data using the following equation:

$$R_m = 6/(\rho_t \, Sa) \tag{3}$$

where ρ_t is the true density (g/m^3) and Sa is the surface area of the powder (m^2/g).

The thermal behavior of the powders was investigated at a heating rate of 10°C/min in flowing air using a Netzch STA449C Jupiter DTA/TGA/DSC instrument. Gas-sensing experiments were carried out in a stainless steel sample holder apparatus equipped with a resistance heater connected to a programmable temperature controller. The sample holder can accommodate up to eight samples for simultaneous electrical resistance measurements. An inlet and an outlet were provided to enable the selected test gases to flow into and out of the sample holder. A Hewlett-Packard data acquisition system, HP 34970A combined with a multiplexer HP34901A and HP Benchlink data logger software was used to collect the data. The gas flow was controlled using mass flow controllers and a 4-channel readout from MKS instruments. A Type K thermocouple placed close to the sensor chip indicated the operating temperature. The electrical resistance of each sensor element was measured in air (R_a) and in the sample gas (R_g), (in this case CO, CH_4, C_3H_8, C_2H_5OH), over a temperature range of 200°C to 550°C. For resistance measurements a load resistance (R_L) was connected in series with the sensor and a circuit voltage (∼5 volts) was applied across them. The resistance of the sensor, R_{Sample}, was obtained by measuring the voltage drop across the standard load resistance using the following equation:

$$R_{Sample} = (V_c/V_{out} - 1) \cdot R_L \tag{4}$$

where R_L denotes the load resistance value (ranging from 10 KΩ to 1 MΩ), V_c is the applied voltage (5 V) and V_{out} is the voltage drop across the load resistance. Gas sensitivity, S, at a particular temperature was evaluated using the relationship, $S = R_a/R_g$. For gas sensitivity measurements, the sample was heated to a chosen temperature where it remained for the duration of the test. At this particular temperature, the resistance was measured at various concentrations (100–1000 ppm) of the test gas in dry air. First, air was run for about 10–20 min to establish a baseline by measuring the sample resistance every 10 or 30 s depending on how fast the sensor responds. Thereafter, 100–1000 ppm of the test gas (e.g., CO, CH_4, C_3H_8, or ethanol) in dry air was run for a fixed length of time (5 or 10 min) while resistance of the samples was measured every 10 or 30 s. This was followed by resistance data measurements in air every 10 or 30 s for a period of 10 min. A constant gas flow rate of 120 sccm was maintained and the flow rates were adjusted for both air and the test gas accordingly to obtain the desired concentrations.

3. Results and discussions

3.1. X-ray diffraction and thermal analysis studies

Fig. 2 shows typical X-ray diffraction (XRD) patterns of tin oxide powders calcined at 550°C for two hours. The

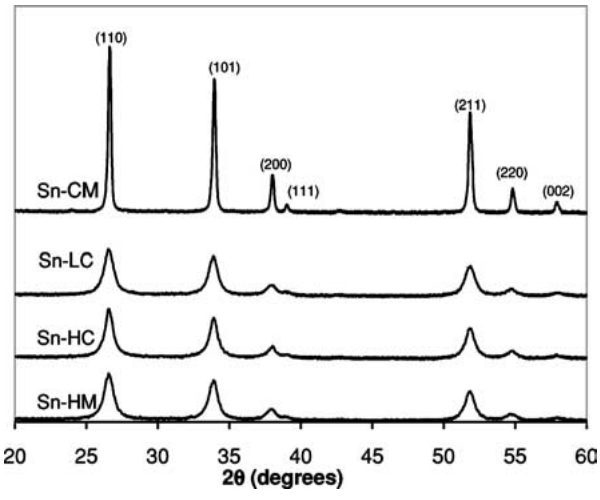

Figure 2 XRD patterns of tin oxide powders calcined at 550°C for 2 h.

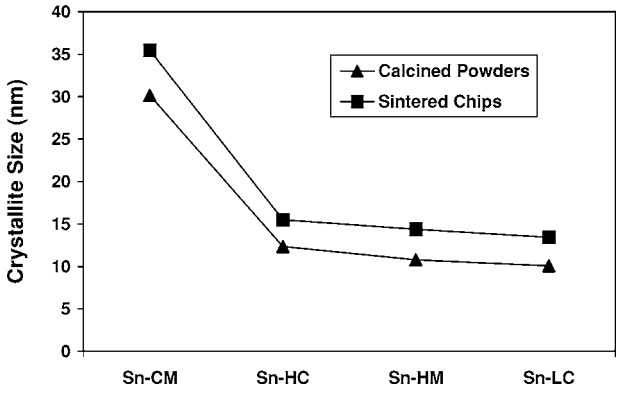

Figure 3 Crystallite sizes of calcined powders & sintered chips calculated from XRD data.

calcined powders displayed only the cassiterite phase. Compared to the commercial powders, the XRD patterns of the powders prepared in-house by the three precipitation methods displayed relatively broader diffraction peaks, indicative of smaller grain/crystallite size. The crystallite sizes (R_x values) of the calcined tin oxide powders calculated from the [110] XRD peak using the Scherrer formula are shown in Fig. 3. It is clear that the tin oxide powders synthesized via chemical processing routes (i.e., Sn-HC, Sn-HM and Sn-LC) provide substantially smaller grain/crystallite sizes (R_x Values) compared to those obtained from the commercial source (Sn-CM). For gas sensor applications, a smaller particle size is desirable as it provides a greater surface-to-bulk-volume ratio resulting in increased adsorption of gases at the sensors surface leading to enhanced sensitivity of the gas sensors. The chemically precipitated powders (Sn-LC and Sn-HM) synthesized using dilute solutions of precipitating agents (NH_4OH and urea, respectively) provide finer powders with grain sizes of 10.1 nm and 10.8 nm respectively, whereas Sn-HC powders prepared using higher concentration NH_4OH as a precipitating agent, produced slightly larger grain size powders (12.35 nm in size). Compared to the chemically processed materials, powders obtained from a commercial source exhibited much larger crystallite size (30.15 nm). Although all of the powders in this study were calcined at 550°C for two hours, the relatively large crystallite sizes obtained for the commercial

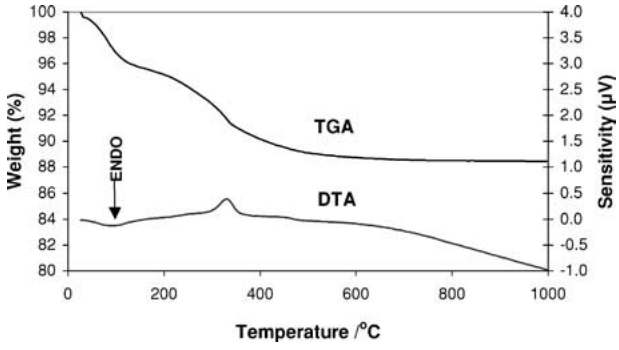

Figure 4 The DTA and TGA plots for Sn-HM dried precipitates.

powders indicate that synthesis and processing conditions, different from those used in-house for the production of precursor powders, may have been used by the commercial supplier.

Fig. 4 shows a typical simultaneous DTA/TGA plot for as-dried powders produced in-house via precipitation methods. The TGA curve depicts a substantial weight loss with increasing temperature to 550°C due presumably to the loss of physically adsorbed water and elimination of ammonia. However, little weight loss in the TGA curve is observed above 550°C, indicating completion of reactions involving a weight change. The DTA curve showed a broad endothermic peak at about 100°C due to the evaporation of physically adsorbed water. An exothermic peak around 330°C is related to the decomposition of NH_4^+ in the powder.

The sensor elements were printed using pastes that were made from the calcined powders produced via the above four methods. The XRD patterns of the sensor chips sintered in air at 725°C for 10 min are shown in Fig. 5. The calculated crystallite sizes (R_x values) for these sensor chips are also shown in Fig. 3. As expected, the high sintering temperature used for the firing of the sensor chips (725°C for 10 min) resulted in grain size growth of the calcined powders. Compared to calcined powders, the sintered chips exhibit 10–30% increase in grain size. The XRD patterns of the sintered sensor chips also displayed XRD peaks arising from the alumina substrate. This occurred because the sensor

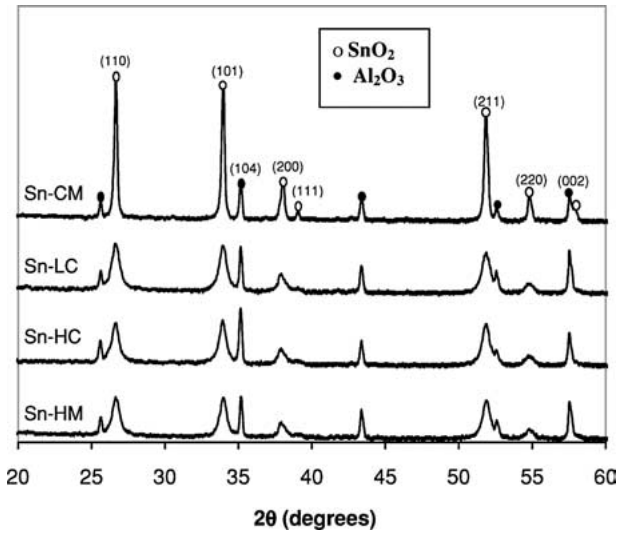

Figure 5 XRD patterns of sintered SnO_2 thick-film sensor chips.

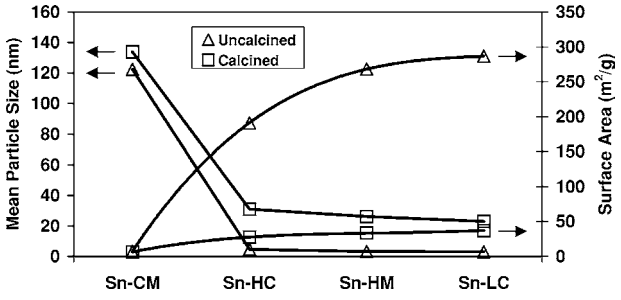

Figure 6 Specific surface area & particle size of calcined and uncalcined powders.

element did not fully cover the alumina substrate and a small part of the alumina was exposed to XRD.

3.2. Surface area measurements and transmission electron microscopy (TEM)

Surface area measurements were performed using the BET method on powders produced via the above four processing routes. Both the calcined (550°C for 2 h) and uncalcined (dried at 135°C for 12 h) powders were used for surface area measurements. Data on the powder surface area measurements and the mean grain size, calculated using Equation 3 are displayed in Fig. 6. As shown in Fig. 6, both the calcined and as-dried powders from the commercial source exhibit a small surface area ($\leq$7.0 m^2/g) and a fairly large grain size (>120 nm), whereas, as-dried and calcined powders produced via chemical precipitation routes exhibited much larger surface areas and smaller grain sizes. The uncalcined powders, Sn-LC and Sn-HM precipitated from dilute solution exhibited surface area values $\geq$268 m^2/g and very small particle size (<3.5 nm). The data also indicates that the calcination of these powders at 550°C for two hours results in almost an order of magnitude reduction in both the surface area and the particle size of the powders. On the other hand, the uncalcined and calcined Sn-HC powders provided relatively smaller surface areas of 191 m^2/g and 27.7 m^2/g, respectively.

Fig. 7a and b show the TEM micrographs of the uncalcined and calcined Sn-LC powders respectively. The

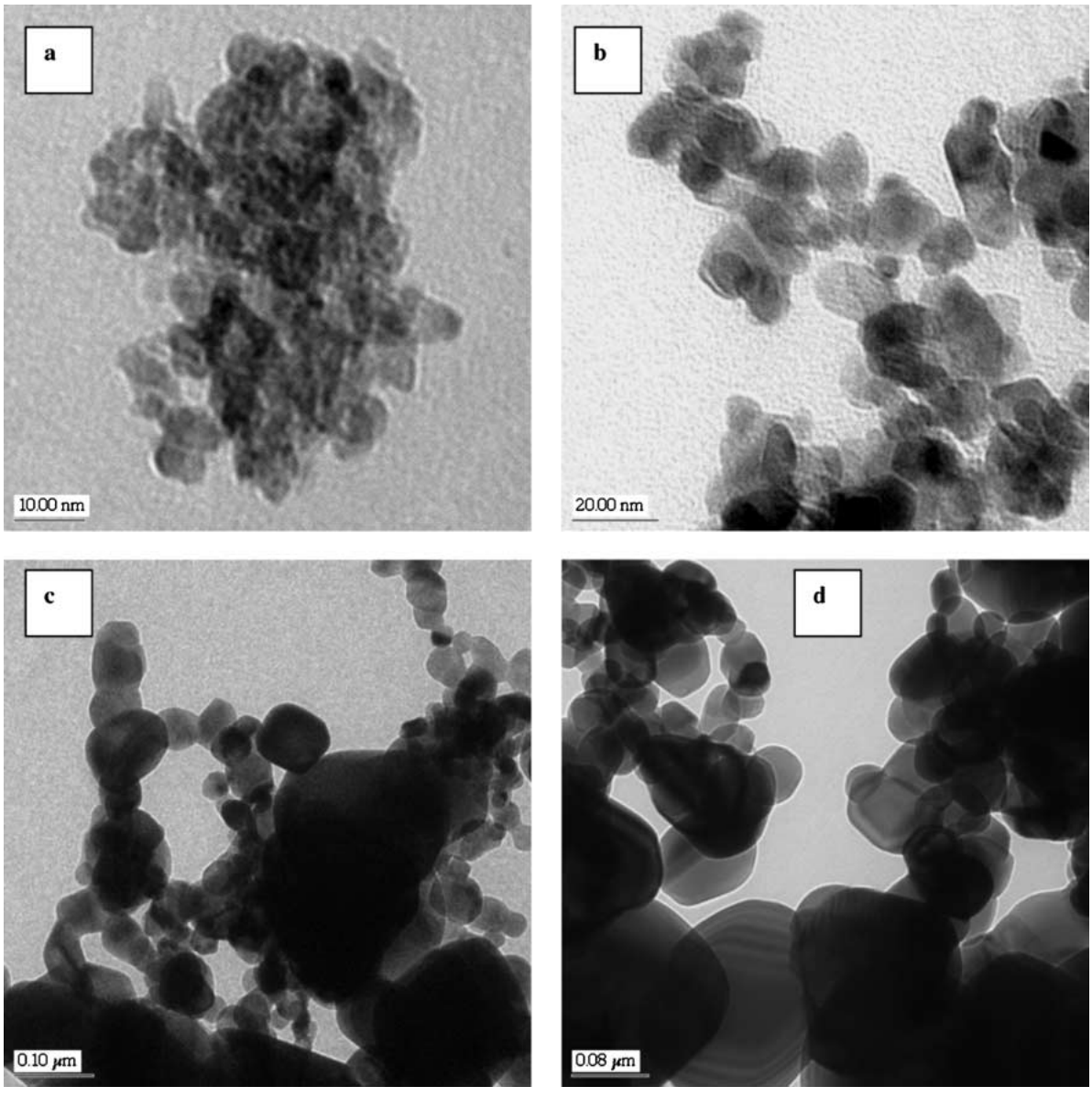

Figure 7 TEM micrographs of the powders: (a) Sn-LC uncalcined, (b) Sn-LC calcined at 550°C/2 h, (c) Sn-CM uncalcined, and (d) Sn-CM calcined powders.

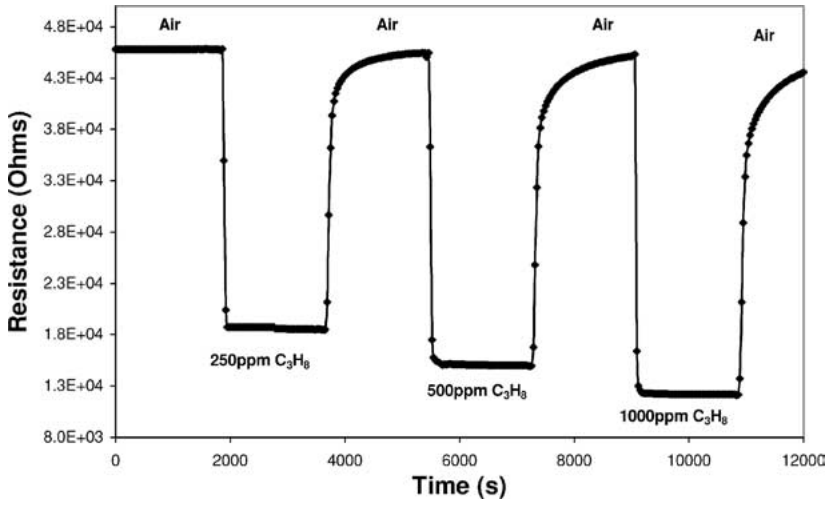

Figure 8 Typical response plot and sensitivity data for SnO_2 sensors (Sn-LC at 500°C).

uncalcined Sn-LC powder displayed fairly small grain sizes ranging from 4–8 nm. The grain size increased to 10–20 nm upon calcination of these powders at 550°C for two hours. In contrast, the TEM of the uncalcined and calcined commercial powders, Fig. 7c and d, respectively, showed relatively much larger grains ranging from 100–150 nm in size. The grain size values for these samples obtained from TEM micrographs are very similar to those calculated from surface area measurements as shown in Fig. 6.

3.3. Electrical conductance and sensitivity data

A typical response plot in air and propane for thick-film gas sensors produced from the above four precursor powders is shown in Fig. 8. The sensitivity, "*S*" of the gas sensors was obtained from the ratio of the resistance in air to that in a reducing gas e.g., propane ($S = R_{air}/R_{gas}$) using response plots similar to Fig. 8. As expected, the sensitivity of the sensor increases with an increase in the propane gas concentration, which is typical behaviour for *n*-type semiconductor gas sensors. The high sensor resistance in air is due to the extraction of electrons from the sensor surface by the adsorbed oxygen. The sensor resistance is, however, lowered when exposed to a reducing gas, e.g., CO, CH_4, C_3H_8 or C_2H_5OH, due to the oxidation of the reducing gas at the sensor surface, releasing electrons back into the semiconductor material. Fig. 9 shows the influence of the powder processing method on the sensitivity of the gas sensors at various temperatures when exposed to 500 ppm ethanol in dry air. These sensors were sintered at 725°C for 10 min. Compared to commercial material, sensors produced from the powders processed in-house via chemical precipitation routes exhibited substantially higher sensitivity to ethanol. This could be due to the higher surface area or smaller particle size observed for the powders processed in-house. The peak sensitivity of the sensors also appears to be influenced by the powder processing method. For example, samples Sn-LC and Sn-HM displayed the highest sensitivity at ~350°C, whereas, sensors made from Sn-HC and Sn-CM powders exhibited peak sensitivity at ~400°C.

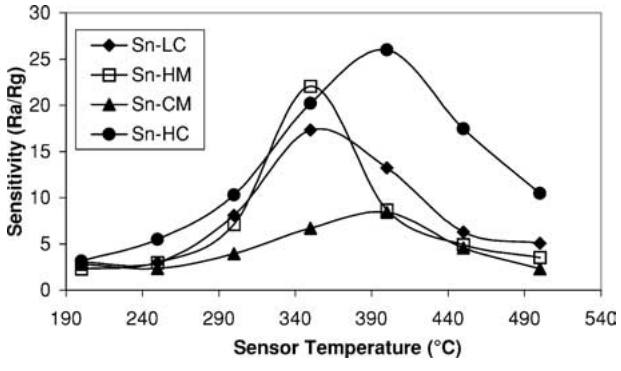

Figure 9 Effect of precursor powders on the sensitivity of gas sensors in 500 ppm ethanol in dry air.

Sensors produced from Sn-HC powders showed the highest sensitivity ($S \approx 26$) in ethanol. No discernable correlations however, could be found with regards to the influence of the powder processing method and the peak sensitivity of the sensors. For example, the sensors produced from Sn-LC powders (and not the Sn-HC samples) showed the highest sensitivity in 500 ppm methane ($S \approx 2.7$ at 450°C) and 500 ppm CO ($S \approx 5.7$ at 425°C) gas environments.

Fig. 10 shows the sensitivity data at various temperatures in 500 ppm propane for Sn-HM sensors sintered

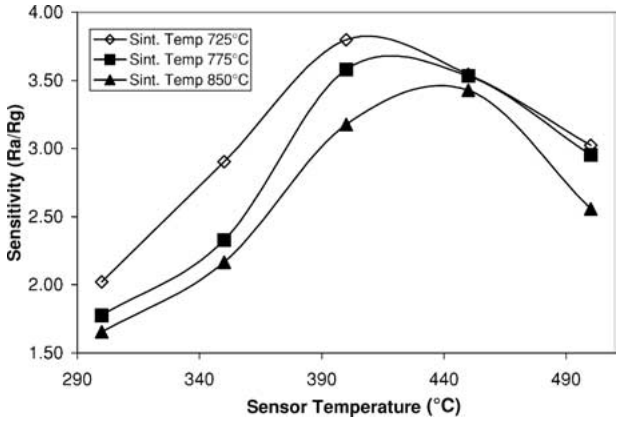

Figure 10 Sensitivity data in 500 ppm propane for Sn-HM samples sintered at 725, 775 and 850°C respectively, for 10 min.

for 10 min at 725, 775 and 850°C respectively. It can be seen that the sensitivity of the sensors decreased with an increase in sintering temperature. This could be attributed to a slight increase in the crystallite size with an increase in sintering temperature, as observed from the XRD data. The peak sensitivity temperature also appears to shift towards a higher value with an increase in sintering temperature. For example, Sn-HM samples sintered at 725°C showed peak sensitivity in propane at ∼400°C, whereas those sintered at 850°C displayed peak sensitivity at ∼450°C. The samples sintered for longer time periods generally exhibited lower sensitivity values in propane.

3.4. Effect of Pd-dopant

The addition of noble catalytic metals (e.g., Pd, Pt) is known to increase the sensitivity of tin oxide-based gas sensors towards reducing gases. Sn-CM and Sn-LC powders produced in this study were doped with 0.5–1 mol% Pd and the influence of Pd dopant on the sensitivity of the gas sensors in propane and ethanol was studied. Fig. 11 shows the sensing behaviour of Pd-doped Sn-CM samples in 500 ppm ethanol in air at various temperatures. Compared to undoped material the sensitivity to ethanol increased with the addition of Pd dopant at lower temperatures. The peak sensitivity also shifted towards lower temperatures with an increase in Pd concentration. At higher temperatures, however >400°C, the undoped material exhibited slightly higher sensitivity to ethanol. A similar shift in peak sensitivity and an increase in sensitivity at lower temperatures was also observed in propane gas. Compared to undoped samples, Pd-doped sensors exhibited a large (up to an order of magnitude) increase in resistance in air at temperatures <400°C. The Pd-doped samples also displayed a slight increase in resistance values (compared to undoped material) in a reducing gas, however, the magnitude of the resistance increase in a reducing gas was substantially lower, resulting in a net increase in the sensitivity of the gas sensors. It has been proposed [19–21] that doping of tin oxide with Pd catalyst results in electronic interaction in which gas adsorption on the catalyst removes electrons from the catalyst which, in turn, removes electrons from the supporting semiconductor, thus controlling intergranular resistance and hence, the sensitivity of the gas sensors.

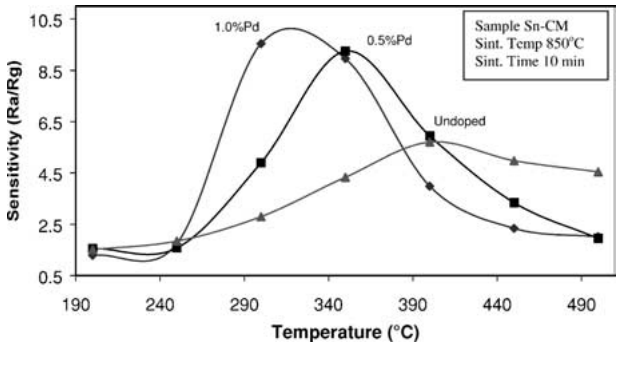

Figure 11 Effect of Pd dopant on the sensitivity of Sn-CM sensors in 500 ppm ethanol in dry air.

3.5. Response and recovery time data

The sensors were exposed to 500 ppm of carbon monoxide, methane, propane and ethanol gas in dry air at various temperatures and the response and recovery times were calculated from response plots similar to that shown in Fig. 8. The response time is defined here as the time it takes for the conductance of the gas sensor to increase to 90% of the maximum conductance when 500 ppm of a reducing gas is introduced into an environment of air. The recovery time is the time required for 90% reduction in conductance when the reducing gas is turned off and air is re-introduced into the chamber (i.e., time to reach 10% of maximum conductance value in a reducing gas). The conductance data for these experiments was recorded every 10 s. Both the response and recovery data for these sensors (in Table I) show strong dependence on the method of processing precursor powders, sensor operating temperature, and gas composition. For example Sn-LC samples prepared from precursor powders synthesized via the precipitation of dilute solutions and sintered at 850°C for 10 min provided a response time of ∼10–15 s at 450°C in 500 ppm methane, whereas sensors produced from commercial powders (Sn-CM) under the same conditions exhibited a response time of ∼40 s. It appears that the sensors made from the precursor powders having smaller particle sizes provide relatively shorter response times. As noted above, compared to commercial powders Sn-LC powders exhibited substantially smaller particle sizes. Also, Sn-LC sensors in 500 ppm propane showed response and recovery times of 60 and 330 s respectively at an operating temperature of 350°C. However, at 450°C the same samples exhibited response and recovery times of 25 and 40 s, respectively. Doping the sensors with Pd generally had a stronger influence on recovery time rather than response time. For example, Sn-CM sensors displayed a response and recovery time of 40 and 120 s, respectively when operated at 450°C and exposed to 500 ppm of propane gas in dry air. However, Sn-CM samples doped with 0.5% Pd showed a response and recovery time of 40 and 50 s respectively, under same operating conditions. Similarly, un-doped Sn-LC samples under the same operating conditions showed response and recovery time values of 25 and 40 s, respectively, whereas the Pd-doped Sn-LC samples exhibited response and recovery times of 20 and 25 s, respectively. It appears that

TABLE I Response and recovery time data in 500 ppm of test gas

Sample I.D	Sensor temperature (°C)	Test gas	Response time (s)	Recovery time (s)
Sn-LC	450	CH_4	10–15	40
Sn-CM	450	CH_4	40	110
Sn-LC	350	C_3H_8	60	330
Sn-LC	450	C_3H_8	25	40
Sn-CM	450	C_3H_8	40	120
Sn-CM + 0.5% Pd	450	C_3H_8	40	50
Sn-LC + 0.5% Pd	450	C_3H_8	20	25

doping the sensors with Pd helps improve the kinetics of oxidation more favourably than the reduction processes at the surface of gas sensors. The response time of the gas sensors also showed a strong dependence on the composition of the gas or the gas environment. For example, at 400°C, Sn-HM sensors (that were sintered at 725°C for 10 min) in the presence of 500 ppm of CO, ethanol, propane and methane exhibited response times of 15, 20, 40 and 120 s, respectively.

4. Conclusions

The powder synthesis methods and processing conditions used in this study appear to have a strong influence on the morphology and microstructural properties of the powders used to fabricate sensor elements. The as-synthesized and dried precursor powders produced by the three precipitation methods used in this study provided powders having very high surface areas (>190 m^2/g) and small particle sizes (3–4.5 nm). Calcination of these powders at 550°C for 2 h provided single-phase tin oxide with almost an order of magnitude reduction in surface area and particle size values. However, these calcined, precipitated powders exhibit surface area values that are still 7–8 times larger than those exhibited by commercial powders. TEM studies of the powders also confirmed small (nano) particle sizes as calculated from surface area measurements. The relatively larger particle/crystallite size and smaller surface area observed for the commercial powders suggests that most likely different processing or heat treatment conditions than those applied in this study were used by the commercial supplier to produce their powders. The sensitivity of the sensors toward various gases (e.g., CO, CH_4, C_3H_8, C_2H_5OH) was found to be dependent on the powder synthesis method as well as the gas concentration, gas composition and sensor temperature. The peak sensitivity of these sensors also showed dependence on the powder synthesis and processing conditions. For example, in 500 ppm ethanol, Sn-LC and Sn-HM samples displayed the highest sensitivity at ∼350°C, whereas sensors made from Sn-HC and Sn-CM powders exhibited peak sensitivity in ethanol at ∼400°C. The response and recovery times for these sensors also showed strong dependence on the method used to synthesize tin oxide precursor powders, sensor operating temperature, doping of the powders with Pd catalyst, as well as the gas composition or environment that the sensors were exposed to.

Acknowledgements

The authors gratefully acknowledge the financial support for this work from the Natural Resources Canada Program on Energy Research and Development (NRCan-PERD). The technical support by Mr. George McDonald, of MTL is also very much appreciated.

References

1. S. SAMSON and C. G. FONSTAD, *J. Appl. Phys.* **44** (1973) 4618.
2. J. F. McALEER, P. T. MOSELEY, J. O. W. NORRIS and D. E. WILLIAMS, *J. Chem. Soc.; Faraday Trans.* 1 **83** (1987) 1323.
3. N. YAMAZOE, J. FUCHIGAMI, M. KISHIKAWA and T. SEIYAMA, *Surf. Sci.* **86** (1986) 335.
4. J. TAMAKI, M. NAGAISHI, Y. TERAOKA, N. MIURA and N. YAMAZOE, *ibid.* **221** (1989) 83.
5. P. VAN GELOVEN, M. HONORE, J. ROGGEN, S. LEPPAVUORI and T. RANTALA, *Sensors and Actuators* B **4** (1991) 185.
6. M. EGASHIRA, M. NAKASHIMA, S. KAWASUMI and T. SEIYAMA, *J. Phys. Chem.* **85** (1981) 4125.
7. G. S. DEVI, S. V. MANORAMA and V. J. RAO, *J. Electrochem. Soc.* **145**(3) (1998) 1039.
8. G. S. V. COLES, G. WILLIAMS and B. SMITH, *Sensors and Actuators* B **3** (1991) 7.
9. G. S. V. COLES, S. E. BOND and G. WILLIAMS, *ibid.* **4** (1991) 485.
10. ZHOU, Y. XU, Q. CAO and S. NIU, *ibid.* **41** (1997) 163.
11. K. NOMURA, H. SHIOZAWA, T. TAKADA, H. REUTHER and E. RICHTER, *J. Mater. Sci.; Mater. Electr.* **8** (1997) 301.
12. H. W. CHEONG, J. J. CHOI, H. P. KIM, J. M. KIM and J. M. KIM, *IEEE* (1991) 154.
13. J. L. SOLIS and V. LANTTO, *Physica Scripta* **T69** (1997) 281.
14. KI CHANG SONG and YONG KANG, *Mater. Lett.* **42** (2000) 283.
15. R. MINHAS, Q. ZHOU, A. AHMAD and T. A. WHEAT, in Proceedings of the International Symposium on Environmental Conscious Materials—Ecomaterials (Metallurgical Society of CIM, 2000) p. 545.
16. R. MINHAS, A. AHMAD and T. A. WHEAT, in Proceedings of the Electrochemical Society, Vol. 99-23, 1999, p. 293.
17. B. D. CULLITY, "Elements of X-ray Diffraction," 2nd edn. (Addison-Wesley Publishing, Massachusetts, 1978).
18. S. R. MORRISON, *Sensors and Actuators* **12** (1987) 425.
19. N. YAMAZOE, *ibid.* B **5** (1991) 7.
20. M. SCHWEIZER-BERBERICH, J. G. ZHANG, U. WEIMAR, W. GOPEL, N. BARSAN, E. PENITA and A. TOMESCU, *ibid.* B **31** (1996) 71.
21. L. N. YANNOPOULOS, *ibid.* **12** (1987) 77.

Received 1 April
and accepted 7 July 2003